

Cellular and Molecular Biology

Original Article

CircSCUBE3 promoted ferroptosis to inhibit lung adenocarcinoma progression

Hongye Fu¹, Qiong Zhao^{2*}¹ Zhejiang Chinese Medical University, Hangzhou, Zhejiang 310053, China² Department of Thoracic Oncology, Shulan (Hangzhou) Hospital, Hangzhou, Zhejiang 310022, China

Article Info

Abstract



Article history:

Received: October 24, 2023

Accepted: January 08, 2024

Published: February 29, 2024

Use your device to scan and read the article online



CircRNAs can regulate ferroptosis and affect cancer development and are promising biomarkers and therapeutic targets in lung cancer. circSCUBE3 is expressed in lung adenocarcinoma (LUAD) tissues. In this study, our purpose was to study the role and regulatory mechanism of circSCUBE3 in LUAD ferroptosis. circSCUBE3 was identified to be significantly downregulated in LUAD samples and cell lines. The expression of biomarkers related to lipid oxidation (4-HNE) and ferroptosis (Ptgs2) was both downregulated in LUAD tissues, suggesting the ferroptosis resistance in LUAD. Erastin, a ferroptosis inducer, was used to stimulate the LUAD cells for 48 h. The cell viability, 4-HNE and Ptgs2 level of LUAD cells were decreased by exposure to erastin while the expression of circSCUBE3 was not significantly altered. We then overexpressed circSCUBE3 in LUAD cells and found it decreased the GSH level and GSH/GSSG ratio in LUAD cells. CircSCUBE3 might serve as an independent factor of ferroptosis and may induce ferroptosis in LUAD by inhibiting GSH synthesis. The loss-of-function experiments were conducted, and circSCUBE3 deficiency reversed the erastin-induced reduction in cell viability, GSH level, GSH/GSSG ratio, mitochondrial membrane potential and elevation in MDA content, Ptgs2, 4-HNE expression as well as lipid ROS production. CircSCUBE3 negatively regulated GPX4 expression in LUAD cells, and the silencing of GPX4 counteracted the impact of circSCUBE3 deficiency on LUAD cell viability as well as ferroptosis, suggesting that circSCUBE3 regulated the GPX4-mediated GSH synthesis in LUAD. CircSCUBE3 was to bind to CREB, which activated the transcription of GPX4. CircSCUBE3 negatively regulated GPX4 expression by competitively interacting with CREB. In the tumor-bearing mouse models, circSCUBE3 silencing promoted tumor growth and reversed the erastin treatment-induced inhibition on tumorigenesis *in vivo*. In conclusion, circSCUBE3 inhibited LUAD development by promoting ferroptosis via the CREB/GPX4/GSH axis, which might provide a novel option for the LUAD targeted therapy.

Keywords: CircSCUBE3, Ferroptosis, GPX4, Lung adenocarcinoma

1. Introduction

Lung cancer (LC) is a highly aggressive malignancy and the leading cause of cancer death globally [1]. Lung adenocarcinoma (LUAD) is the most prevalent LC subtype, followed by squamous-cell carcinomas [2]. The advance in diagnosis and therapy including surgery, radiotherapy, and targeted therapy contributes to the improvement of clinical outcomes. However, the challenges in early detection, high metastasis rates, and therapy resistance threaten the survival of patients, and the five-year survival rate in patients with LUAD is under 20% [3-5]. Exploration of the underlying mechanism in LUAD carcinogenesis and identification of promising therapeutic targets is of significant value for LUAD treatment.

Ferroptosis dysfunction is involved in various diseases including lung cancer. Ferroptosis is regarded as an iron-dependent and non-apoptotic type of regulated cell death featured by lipid peroxide accumulation [6]. The inactivation of the cellular antioxidant system with lipid reactive oxygen species (ROS) accumulation is a critical cause of

ferroptosis [7]. GPX4 is regarded as a central downstream ferroptosis modulator by clearing ROS as well as maintaining redox homeostasis. Glutathione (GSH) is a cofactor of GPX4 and is oxidized to GSSG as a byproduct when GPX4 is combined with lipid peroxidation to reduce lipid hydroperoxides to lipid alcohols [8]. The deficiency of GSH can inactivate GPX4. GPX4 inhibition can also be achieved through pharmacological or genetic means can lead to ferroptosis [9]. In recent years, increasing attention has been attracted on the role of ferroptosis in different diseases, including in cancer therapy [9, 10]. A previous study has unveiled that the CREB facilitates the transcription of GPX4 to inhibit ferroptosis in LUAD [11]. Therefore, the inhibition of GPX4 transcription in LUAD cells is a promising target for the therapy of LUAD.

Circular RNAs (circRNA) refer to a type of covalently closed single-stranded non-coding RNAs without 5' caps and 3' poly(A) tails and are produced via the back-splicing of their pre-mRNAs. Increasing evidence has shown that the dysregulation of circRNAs is associated with the

* Corresponding author.

E-mail address: zhaoqiong_shulan@163.com (Q. Zhao).Doi: <http://dx.doi.org/10.14715/cmb/2024.70.2.23>

progression of various diseases, including LUAD [12, 13]. Studies have shown that circRNAs serve as critical regulators of gene expression via diverse mechanisms, including as acting as transcriptional regulators interacting with miRNAs and RNA binding proteins (RBPs) [14, 15]. For example, circXPO1 is reported to facilitate LUAD cell proliferative capacity and tumor growth by interacting with IGF2BP1 to enhance CTNNB1 mRNA stability [16]. Circ-ENO1 promotes the proliferation, migration and glycolysis of LUAD cells by binding to miR-22-3p to upregulate ENO1 [17]. CircDCUN1D4 is revealed to repress cell invasion and glycolysis in lung cancer by interacting with HuR to enhance TXNIP mRNA stability [18]. Moreover, circRNAs are indicated to affect the process of ferroptosis by regulating the genes or proteins associated with ferroptosis in direct or indirect ways [19]. Based on the GEO datasets, hsa_circRNA_104099 (circSCUBE3) is found lowly expressed in the LUAD tissues. However, the role of circSCUBE3 in LUAD progression remains unexplored.

In the current study, we intended to explore the effects and underlying mechanisms of ferroptosis in LUAD. Loss-of-function assays were conducted to explore the impact of circSCUBE3 deficiency on the viability and ferroptosis-related biomarkers in LUAD cells. Mechanically, we hypothesized that circSCUBE3 might affect ferroptosis in LUAD by regulating GPX4. The findings of this study might deepen our understanding of the role of circSCUBE3 in the LUAD progression and provide a novel candidate for LUAD-targeted therapy.

2. Materials and methods

2.1. Patient specimens

The LUAD tumor tissues and adjacent normal tissues were collected during surgery from LUAD patients at our hospital. The tissue specimens were confirmed by pathologists and stored at -80°C before use. The study acquired the approval of the Ethics Committee of our hospital and the written informed consent was provided by all patients enrolled in this study.

2.2. Cell culture and treatment

Human LUAD cell lines (A549, H1975) and bronchial epithelial cells (BEAS-2B) were obtained from The American Type Culture Collection and incubated in RPMI-1640 medium containing 10% fetal bovine serum (FBS, Gibco, USA) and 100 U/mL penicillin and 0.1 g/mL streptomycin at 37°C with 5% CO_2 . For erastin treatment, cells were stimulated by 10 μM of erastin for 24 h.

2.3. RNase R treatment

Total RNA was collected from the A549 and H1975 cells maintained at 37°C in the presence or absence of 3 U/ μg RNase R (Sigma-Aldrich, USA) for 0.5 hours. Then the RNA was purified followed by qRT-PCR analysis.

2.4. Actinomycin D (ActD) assays

A549 and H1975 cells were stimulated by 2 $\mu\text{g}/\text{ml}$ ActD (Sigma-Aldrich, USA) for 0, 6, 12, 18 and 24 h. Then total RNA in the treated cells was collected and subject to qRT-PCR analysis.

2.5. Cell transfection

ShRNAs targeting circSCUBE3 (sh-circSCUBE3),

GPX4 (sh-GPX4) or CREB (sh-CREB) and matched negative controls (sh-NC) were designed and synthesized by Genechem (Shanghai, China). For circSCUBE3 overexpression, the full length of circSCUBE3 was cloned into pCDNA3.1 overexpression vectors (GENERAY BIOTECH, Shanghai). A549 and H1975 cells were grown into 6-well plates before transfection with indicated vectors for 48 hours with the Lipofectamine 2000 (Invitrogen, MA, USA) in accordance with the producer's protocol.

2.6. Cell viability

A549 and H1975 cell viability was examined using a CCK-8 assay kit (GLPBIO, Montclair, CA, USA). Cells (1×10^4) were grown into 96-well plates before incubation for 48 hours. After the addition of CCK-8 reagent (10 μL) into each well, cells were maintained for another two hours. A microplate reader (BioTek, VT, USA) was applied to determine the absorbance at 450 nm.

2.7. Quantitative reverse transcription PCR (qRT-PCR)

TRIzol (Invitrogen; Thermo Fisher, USA) was used for total RNA isolation from cells and tumor tissues. The PrimeScript RT Reagent Kit (TaKaRa, Japan) was used for reverse transcription according to the producer's protocol. qPCR was conducted with a Hieff qPCR SYBR Green Master Mix kit (Yeasen, China). The relative quantification of RNA expression was calculated by the $2^{-\Delta\Delta\text{Ct}}$ method with GAPDH as the internal control. The primer sequences were shown below: circSCUBE3: F: 5'-CGTGTGATGACACAGAGCAG-3'; R: 5'-TGTTCTGGCAGATAGCATCG-3'; SCUBE3: 5'-GGATCAACTTCAAGACAAGC-3'; R: 5'-GCTCATAGTCCTCATCATAGG-3'; Ptg2: F: 5'-TCAGCCATACAGCAAATCC-3'; R: 5'-TATACTGGTCAAATCCCACAC-3'; GAPDH: F: 5'-TCATTTCTGGTATGACAACGA-3'; R: 5'-GTCTACTCCTTGGAGGCC-3';

2.8. Measurements of malondialdehyde (MDA), 4-HNE concentration and GSH/GSSG ratio

MDA and 4-HNE content in the treated A549 and H1975 cells were measured using commercial kits from Abcam (MDA kit, Cat. No ab118970, 532 nm; 4-HNE kit, Cat. No ab238538, 450 nm) using a microplate reader (BioTek). GSH (Cat. No. BC1175, Solarbio, China) and GSSG assay kits (Cat. No. BC1180, Solarbio) were applied for the measurement of the GSH level as well as the GSH/GSSG ratio.

2.9. Lipid reactive oxygen species (ROS) detection

The lipid ROS levels in the treated LUAD cells were detected with fluorescent BODIPY 581/591 C11 probes (Invitrogen, USA). Cells were grown into the 3.5 cm plates and pretreated with transfection vectors or erastin. Then cells were cultured with the BODIPY-C11 at 1.5 μM for 20 min, followed by PBS washing thrice. Results were recorded with a Leica microscope and subject to flow cytometry analysis.

2.10. Mitochondrial membrane potential assay

An Enhanced mitochondrial membrane potential assay kit with JC-1 (Beyotime) was applied to measure the mitochondrial membrane potential in accordance with the producer's protocol. The treated A549 and H1975 cells were

incubated for 24 hours in a six-well plate (3×10^5 cells/well). Then cells were stained with 1 mL of JC-1. The results were analyzed by flow cytometry with the excitation wavelength at 488 nm and the emission wavelength at 529 and 590 nm for monometric and J-aggregate JC-1, respectively.

2.11. RNA immunoprecipitation (RIP)

The binding between circSCUBE3 and CREB was explored using a Magna RIP Kit (Millipore, USA) according to the producer's guidelines. Cells were treated with lysis buffer followed by culturing with magnetic beads loaded with the anti-CREB antibody (Invitrogen), or anti-IgG (abcam) overnight at 4°C. Finally, cells were maintained with proteinase K (Sigma-Aldrich) for 0.5 h at 55°C. RNA extraction was conducted with TRIzol and qRT-PCR was carried out to measure the circSCUBE3 expression in the precipitates.

2.12. RNA pulldown assays

A549 and H1975 cells were processed with lysis buffer and then the cell lysates were incubated with the bio-NC and bio-circSCUBE3 probes (GenePharma, Shanghai, China) overnight at 4°C. Next, the mixture was added with streptavidin magnetic beads (MCE, USA) and maintained for three hours. After washing thrice, the enriched proteins in the complexes were extracted and subjected to western blot.

2.13. ChIP

A549 and H1975 cells (2×10^7) were processed with 1% formaldehyde for 10 min and then sonicated to 150–900 bp for chromatin fragments. Then the protein A/G beads coupled with the anti-CREB (Cat. No. MA1-083, Invitrogen) and negative control anti-IgG antibodies were supplemented and cultured with the lysates overnight at 4°C. Next, the immunocomplexes were eluted and the enrichment of GPX4 promoter fragment binding to CREB was detected by qRT-PCR.

2.14. Western blot

RIPA lysis buffer (Sigma-Aldrich) was applied to isolate total protein from treated cells. Then the concentration of protein was analyzed by a BCA assay. The samples were separated by 10% SDS-PAGE gels and then transferred to PVDF membranes (Merk, Darmstadt, Germany). After blocking with 5% nonfat milk, the membranes were maintained with the anti-CREB (Cat. No. MA1-083, 1:500, Invitrogen), anti-GPX4 (Cat. No. ab125066, 1:1000, abcam) at 4°C overnight with primary GAPDH as a loading control. Then the membranes were cultured at ambient temperature with the secondary antibody for 1 hour. The ECL reagents (Pierce, MA, USA) were used for protein band visualization and ImageJ software was applied for quantification.

2.15. Xenograft tumorigenesis

BALB/c nude mice (5 weeks) were purchased from the Beijing Vital River Laboratory Animal Technology Co., Ltd. (Beijing, China). The procedures of the animal experiment were conducted under the approval of the Ethics committee of our hospital. The animals were randomized into 4 groups, including the sh-NC, sh-circSCUBE3, erastin+sh-NC and erastin+sh-circSCUBE3 groups (6

mice per group) when the tumor size reached 100 mm³. A549 cells (4×10^5) transfected with sh-circSCUBE3 or sh-NC were injected subcutaneously into the mouse right flank. Tumor size was monitored and recorded every three days. Mice were executed at the end of the experiment on day 24. The tumors were excised and weighed. For erastin treatment, mice were intraperitoneally administrated with 15 mg/kg erastin (Selleck Chemicals, Houston, TX, USA) twice per week.

2.16. Immunohistochemistry (IHC)

The tumor samples or adjacent normal tissues obtained from LUAD patients or tumors from mice in each group were immersed in 4% paraformaldehyde, paraffin-embedded and 5- μ m sections were prepared. Then sections were treated using xylene for 15 min and rehydrated in gradient alcohol, the sections were maintained for 10 min at 105°C, and then processed with the citric acid buffer. Next, after PBS washing and treatment with 3% hydrogen peroxide solution, sections were maintained with the 10% normal goat serum for 30 min at 37°C. Subsequently, the samples were cultured with the anti-4-HNE (Cat. No. MAB3249, R&D Systems, USA), anti-Ptgs2 (Cat. No. ab179800, 1:100, abcam), anti-GPX4 (Cat. No. ab125066, 1:250, abcam) at 37°C for two hours. After incubation with the secondary antibody for 60 min, the sections were dyed with hematoxylin for 4 min. Results were observed using an Olympus microscope and scored by two blinded pathologists.

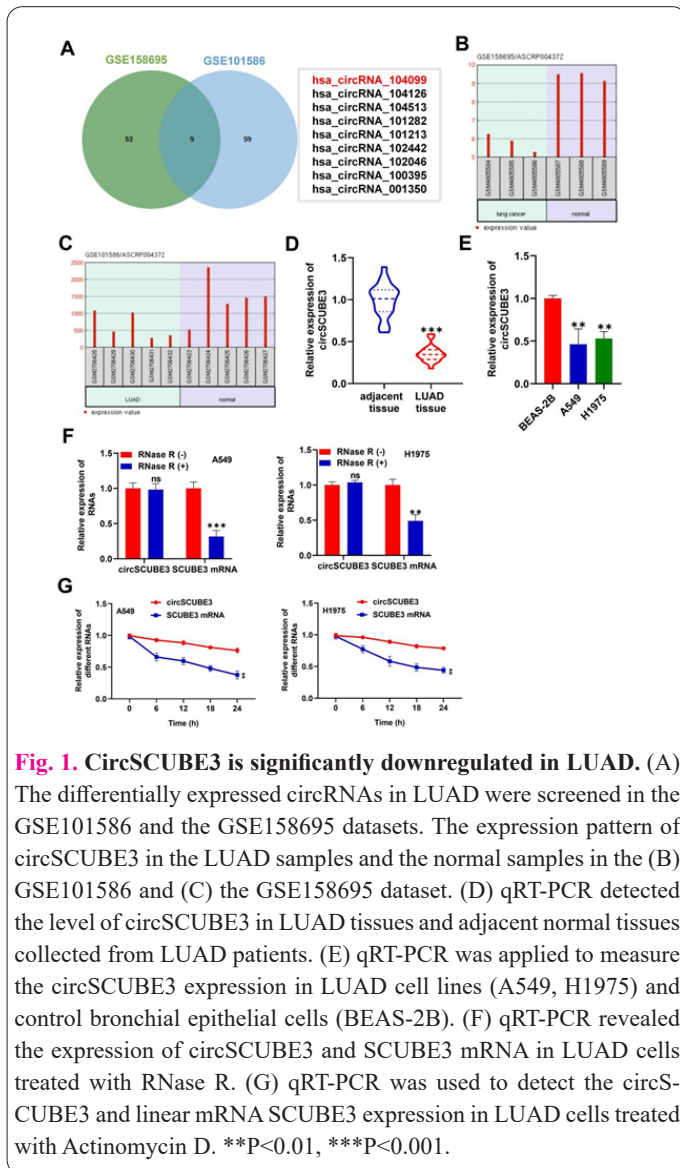
2.17. Statistical analysis

Results are shown as the mean \pm standard deviation (SD). GraphPad prism version 8 was applied for data analyses. Student's t-test was applied for between-group comparisons and one-way ANOVA was used for comparisons among three or more groups. $P < 0.05$ was set as the threshold value.

3. Results

3.1. CircSCUBE3 is significantly downregulated in LUAD

The differentially expressed circRNAs in LUAD were searched on the GEO database. Based on the analysis of the GSE101586 combined with the GSE158695 dataset, 9 differentially expressed circRNAs were screened, among which the role of hsa_circRNA_104099 (circ-Base ID: hsa_circ_0076092, gene symbol: SCUBE3) in the regulation of LUAD has not been reported (Figure 1A). As shown in Figures 1B, C, the circSCUBE3 was lowly expressed in the LUAD tumor specimens relative to the normal adjacent specimens in the GSE101586 and GSE158695 datasets. We further identified that the expression of circSCUBE3 was significantly lower in the LUAD tissues relative to the adjacent normal tissues (Figure 1D). We then analyzed the levels of circSCUBE3 in LUAD cells (A549, H1975) as well as bronchial epithelial cells (BEAS-2B). The results demonstrated the downregulation of circSCUBE3 in LUAD cells in comparison with BEAS-2B cells (Figure 1E). After the RNase R treatment, the SCUBE3 mRNA levels were significantly reduced, while the expression of circSCUBE3 exhibited no evident change, which indicated that circRNA is stable and resistant to the digestion of RNase R (Figure 1F). Moreover, the expression of SCUBE3 mRNA in LUAD cells trea-



ted with Actinomycin D showed significant downregulation, while the circSCUBE3 was not significantly altered, which further suggested that the circRNA was more stable compared with its linear mRNA (Figure 1G).

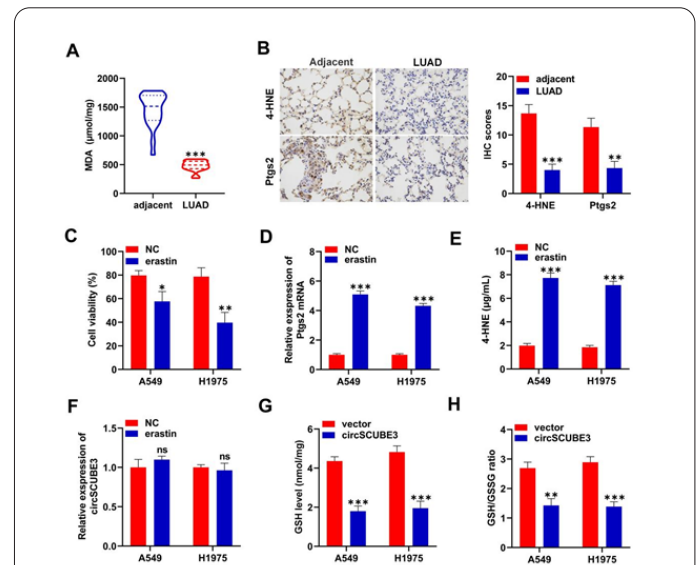
3.2. CircSCUBE3 promoted ferroptosis of LUAD cells

Ferroptosis is regarded as a potential option for anti-cancer treatment. The role of circSCUBE3 in the regulation of ferroptosis in LUAD was investigated. As shown in Figure 2A, the concentration of MDA was reduced in the LUAD tissues relative to the adjacent normal tissues. Then we analyzed the expression of biomarkers related to lipid oxidation (4-HNE) and ferroptosis (Ptgs2). Immunohistochemistry unveiled that both 4-HNE and Ptgs2 were downregulated in LUAD tissues, which indicated the ferroptosis resistance in LUAD (Figure 2B). After the treatment with ferroptosis inducer erastin, the A549 and H1975 cell viability was significantly reduced (Figure 2C), and the levels of Ptgs2 mRNA and 4-HNE concentration exhibited significant elevation in the LUAD cells exposed to erastin (Figures 2D, E), which indicated that the induction of ferroptosis is an alternative for anti-LUAD treatment. In addition, circSCUBE3 levels showed no significant change after the stimulation of erastin in LUAD cells (Figure 2F), while the GSH level and GSH/GSSG ratio were significantly increased by overexpressing circSCUBE3 in

LUAD cells (Figures 2G, H), which suggested that circSCUBE3 might serve as an independent factor of ferroptosis and may induce the ferroptosis in LUAD by inhibiting GSH synthesis.

3.3. CircSCUBE3 deficiency promoted the GSH synthesis and suppressed the LUAD cell ferroptosis

Then we examined the effects of circSCUBE3 on cell ferroptosis in LUAD. CCK-8 assays revealed that the reduced viability of LUAD cells by erastin stimulation was reversed after the transfection of sh-circSCUBE3 into LUAD cells (Figure 3A). The GSH level showed a significant decrease after the erastin treatment and was elevated by silencing circSCUBE3 in erastin-treated LUAD cells (Figure 3B). Moreover, we also demonstrated that circSCUBE3 deficiency rescued the erastin-induced reduction in GSH/GSSG ratio in LUAD cells (Figure 3C). However, the MDA content was elevated in the erastin-stimulated A549 and H1975 cells, and decreased in the erastin+sh-circSCUBE3 group (Figure 3D). The elevation in Ptgs2 mRNA and 4-HNE levels in the erastin-stimulated A549 and H1975 cells was also demonstrated to be reversed after silencing circSCUBE3 (Figures 3E, F). Additionally, we also detected that the erastin treatment caused an increase in lipid ROS level, which was reduced by circSCUBE3 knockdown (Figures 3G, H). Moreover, the erastin decreased the mitochondrial membrane potential of LUAD cells, which was exhibited as the fluorescence shift from red to green. After the transfection of sh-circSCUBE3, the fraction of cells showing red fluorescence was increased,



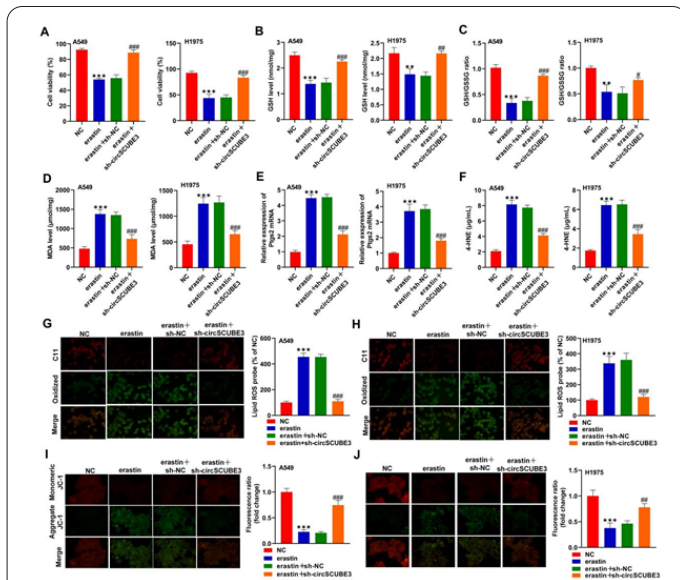


Fig. 3. CircSCUBE3 deficiency promoted GSH synthesis and suppressed the ferroptosis of LUAD cells. (A) CCK-8 assays were conducted to detect the viability of LUAD cells after erastin treatment or circSCUBE3 knockdown. (B) GSH and (C) GSH/GSSG ratio in LUAD cells in each group were examined using commercial kits. (D) MDA content in LUAD cells in indicated groups. (E) Ptg2 mRNA expression in LUAD cells in each group was detected using qRT-PCR. (F) The concentration of 4-HNE in LUAD cells after indicated treatment. (G, H) The lipid ROS level in LUAD cells was measured by immunofluorescence. (I, J) The mitochondrial membrane potential in LUAD cells was examined with JC-1 staining. ** $P < 0.001$, ### $P < 0.001$.

suggesting that circSCUBE3 deficiency decreased the erastin-induced mitochondrial damage (Figures 3I, J).

3.4. CircSCUBE3 regulated GPX4-mediated GSH synthesis

The underlying mechanism of circSCUBE3 to regulate GSH was further investigated. GPX4 is previously reported to regulate GSH to protect cells from ferroptosis. We then explored whether circSCUBE3 regulated GPX4 in LUAD. As shown in Figure 4A, the expression of GPX4 showed significant elevation in A549 and H1975 cells after silencing circSCUBE3, suggesting the positive regulation of circSCUBE3 on GPX4 in LUAD. Then we treated the A549 cells with 10 μM of erastin to induce ferroptosis. Based on the results of rescue assays, we found that the viability of LUAD cells was elevated by silencing circSCUBE3, which was revealed to be reversed after GPX4 knockdown (Figure 4B). Moreover, the GSH level was elevated by silencing circSCUBE3, and GPX4 knockdown restored the GSH level in A549 cells (Figure 4C). Consistently, the increase in GSH/GSSG ratio caused by circSCUBE3 deficiency was counteracted after the transfection of sh-GPX4 in A549 cells (Figure 4D). The MDA content in the A549 cells was decreased by silencing circSCUBE3 and showed significant elevation after GPX4 knockdown (Figure 4E). The Ptg2 mRNA expression reduced by circSCUBE3 deficiency was also demonstrated to be rescued after GPX4 knockdown (Figure 4F). Additionally, the lipid ROS levels in the sh-circSCUBE3 group were significantly lower than those in the sh-NC group, while the GPX4 knockdown was revealed to restore the lipid ROS level compared with the sh-circSCUBE3 group

(Figure 4G). Moreover, according to the result of JC-1 staining, the sh-circSCUBE3 group showed higher mitochondrial membrane potential than the sh-NC group, while the GPX4 silencing significantly reduced the mitochondrial membrane potential to the normal level (Figure 4H). Overall, the results suggested that circSCUBE3 promotes the ferroptosis of LUAD cells by regulating the GPX4-mediated GSH synthesis.

3.5. CircSCUBE3 and GPX4 competitively bound with CREB

CREB has been reported to promote the transcription of GPX4 to suppress ferroptosis in LUAD [11]. We assumed that CERB might regulate GSH via GPX4. The sh-CREB and GPX4 overexpression vectors were cotransfected into A549 and H1975 cells, and we found that the GSH level, as well as the GSH/GSSG ratio in the sh-CREB group, showed an evident decrease relative to the control, while

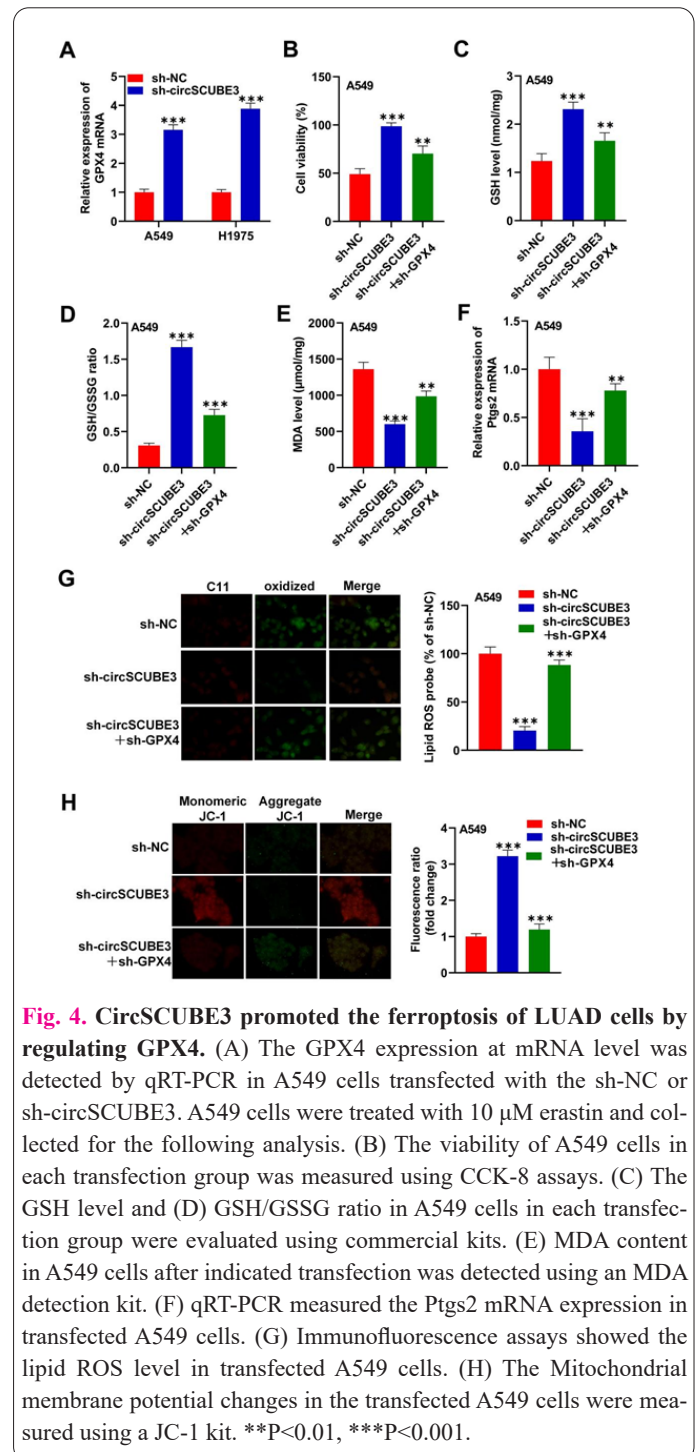
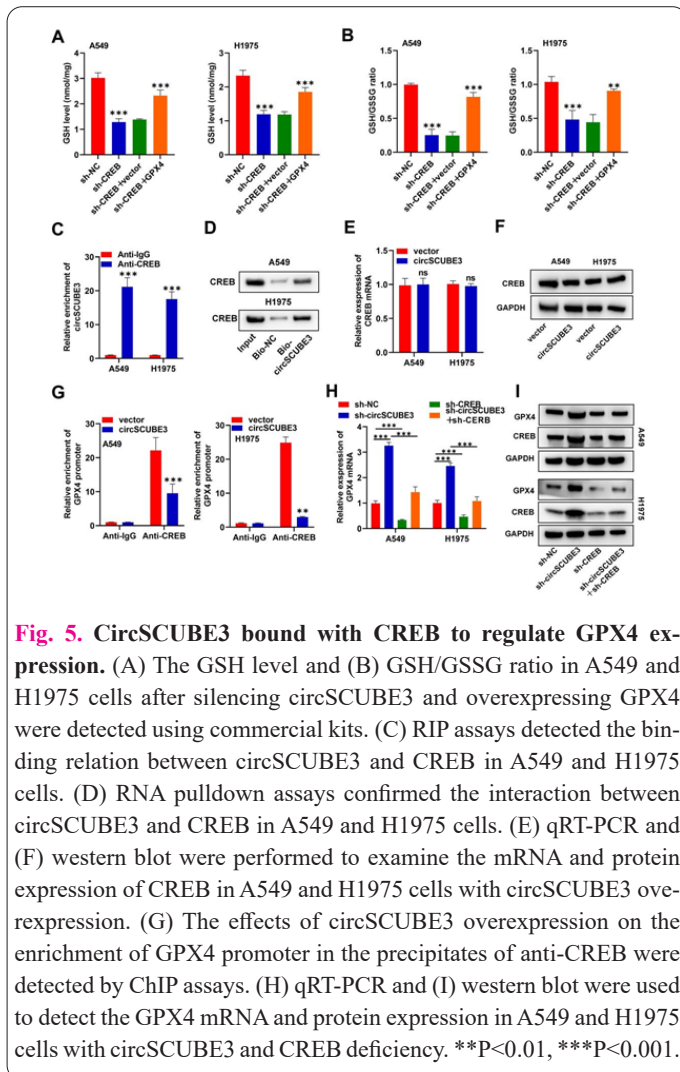


Fig. 4. CircSCUBE3 promoted the ferroptosis of LUAD cells by regulating GPX4. (A) The GPX4 expression at mRNA level was detected by qRT-PCR in A549 cells transfected with the sh-NC or sh-circSCUBE3. A549 cells were treated with 10 μM erastin and collected for the following analysis. (B) The viability of A549 cells in each transfection group was measured using CCK-8 assays. (C) The GSH level and (D) GSH/GSSG ratio in A549 cells in each transfection group were evaluated using commercial kits. (E) MDA content in A549 cells after indicated transfection was detected using an MDA detection kit. (F) qRT-PCR measured the Ptg2 mRNA expression in transfected A549 cells. (G) Immunofluorescence assays showed the lipid ROS level in transfected A549 cells. (H) The Mitochondrial membrane potential changes in the transfected A549 cells were measured using a JC-1 kit. ** $P < 0.01$, *** $P < 0.001$.



that in the sh-CREB+GPX4 group was elevated relative to the sh-CREB group, suggesting that CREB regulated the GPX4-mediated GSH synthesis in LUAD cells (Figures 5A, B). CircSCUBE3 was demonstrated to negatively regulate the GPX4-mediated GSH synthesis to promote ferroptosis in LUAD (Figure 4). We then explored the effects of circSCUBE3 on CREB-mediated GPX4 transcription in A549 and H1975 cells. Based on the results of RIP assays, we found the abundant enrichment of circSCUBE3 in the precipitates in the anti-CREB group in A549 and H1975 cells (Figure 5C). Moreover, the RNA pulldown assays also revealed that the CREB was enriched in the complex of bio-circSCUBE3 in LUAD cells (Figure 5D), which indicated that circSCUBE3 bound with CREB in LUAD cells. However, the regulation of circSCUBE3 on CREB in LUAD cells was explored, and we found that CREB mRNA and protein expression were not significantly affected by circSCUBE3 in LUAD cells (Figures 5E, F). ChIP assays revealed that the GPX4 promoter was enriched in the precipitates in the anti-CREB group, which was significantly decreased by the circSCUBE3 overexpression in LUAD cells, suggesting that the circSCUBE3 decreased the binding between CREB and GPX4 in LUAD cells (Figure 5G). Moreover, GPX4 levels in LUAD cells after silencing circSCUBE3 and CREB were explored, and its mRNA and protein levels were negatively regulated by circSCUBE3 and positively regulated by CREB in A549 and H1975 cells. The elevation in GPX4 levels in LUAD cells caused by circSCUBE3 silencing was reversed by

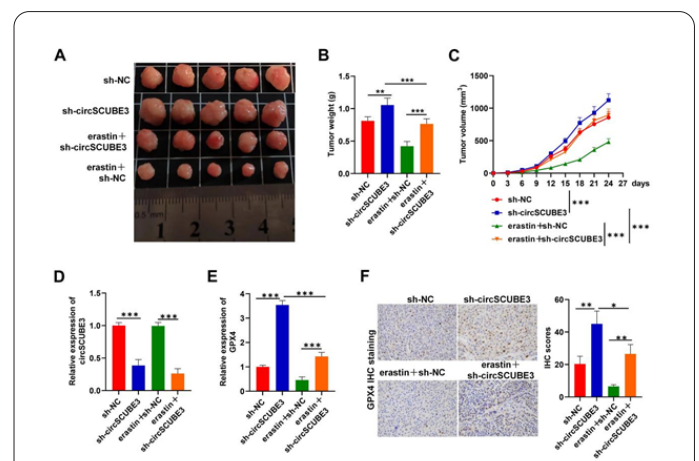
cotransfection of sh-CREB vectors, which suggested that CREB was required in the circSCUBE3-mediated regulation of GPX4 (Figures 5H, I). Overall, these results indicated that circSCUBE3 is bound with CREB to modulate GPX4 expression in LUAD cells.

3.6. CircSCUBE3 suppressed the LUAD tumorigenesis and promoted ferroptosis *in vivo*

Tumor-bearing mouse models were established using A549 cells with the transfection of sh-circSCUBE3 and sh-NC to investigate the effects of circSCUBE3 on tumor growth *in vivo*. Mice were treated with erastin to induce ferroptosis. The results showed that the evidently larger tumor size with circSCUBE3 silencing relative to control, while the erastin treatment was revealed to decrease the tumor size compared with the control. Moreover, we also found that the tumor weight, as well as volume of mice in the erastin+sh-circSCUBE3 group, showed significant elevation relative to the erastin +sh-NC group, which suggested that circSCUBE3 deficiency attenuated the suppressive effects of erastin on LUAD tumorigenesis (Figures 6A-C). Additionally, we detected the expression levels of circSCUBE3 and GPX4 in the collected tumor samples in each group. The expression of circSCUBE3 was confirmed to be decreased in the sh-circSCUBE3 group and showed significant elevation by erastin treatment. The increase in circSCUBE3 expression caused by erastin treatment in mouse tumor tissues was reversed after circSCUBE3 knockdown (Figure 6D). However, the GPX4 expression exhibited the opposite changes in mouse tumor tissues. GPX4 was revealed to be negatively regulated by circSCUBE3 and decreased by erastin treatment. Moreover, the erastin-induced reduction of GPX4 expression of revealed to be rescued after silencing circSCUBE3 (Figure 6E). The immunohistochemistry also showed that the protein levels of GPX4 decreased by erastin treatment were reversed after circSCUBE3 knockdown (Figure 6F).

4. Discussion

Compared with the linear mRNAs, circRNAs are much



more stable and abundant and are promising candidate biomarkers for diagnosis and treatment in LUAD [20, 21]. Resistance to ferroptosis is associated with the progression of diverse diseases, lung cancer included [22]. Increasing evidence has shown that circRNAs are important regulators of ferroptosis in cancer development [23]. In this study, we explored the role and potential regulatory mechanism of circSCUBE3 (hsa_circ_0076092) in LUAD carcinogenesis. We identified the downregulation of circSCUBE3 in LUAD tissue samples and cells. Moreover, we revealed that circSCUBE3 was an independent factor that induced ferroptosis of LUAD cells by inhibiting GSH synthesis. Further analysis showed that circSCUBE3 silencing rescued the erastin stimulation and caused a reduction in cell viability and ferroptosis of LUAD cells. Mechanically, circSCUBE3 regulated GSH synthesis by negatively regulating GPX4. CircSCUBE3 and GPX4 are competitively bound to CREB, and circSCUBE3 overexpression inhibited the CREB-mediated transcription of GPX4. In the tumor-bearing mouse models, we demonstrated the anti-tumor effects of circSCUBE3 on tumorigenesis.

CircRNAs are endogenous biomolecules with tissue- and cell-specific expression profiles, and function as important regulators of gene expression via diverse mechanisms [15, 24]. Energy metabolism alteration is a hallmark of cancer development and circRNAs are indicated to play crucial roles in this process [25]. Multiple circRNAs have been revealed to affect ferroptosis by acting on GPX4 or lipid metabolism or other ferroptosis-related pathways in the cancer progression. For example, circKIF4A inhibits ferroptosis by binding to miR-1231 to upregulate GPX4 in papillary thyroid cancer [26]. CircRNA_101093 suppresses ferroptosis by interacting with FABP3 and induces NAT in LUAD [27]. CircCDK14 inhibits ferroptosis and promotes glioma progression by binding to miR-3938 to upregulate miR-3938 expression [28]. In this work, circSCUBE3 was confirmed to be lowly expressed in LUAD tumor specimens. We also verified that circSCUBE3 was stable and resistant to RNase R digestion. Moreover, circSCUBE3 expression was not evidently altered by the erastin exposure, and circSCUBE3 overexpression was demonstrated to reduce the GSH and GSH/GSSG ratio in the A549 and H1975 cells, suggesting it as an independent factor influencing ferroptosis. Moreover, we found that circSCUBE3 deficiency reversed the erastin-induced reduction in cell viability, alteration in levels of biomarkers of ferroptosis including Ptg2, lipid peroxidation (4-HNE and MDA), glutathione (GSH) levels and GSH/GSSG ratio in A549 and H1975 cells.

Ferroptosis dysfunction is involved in the biological processes including lipid metabolism, iron metabolism and GSH synthesis in various diseases [29-31]. GPX4 is reported to protect cells from ferroptosis by regulating GSH. GPX4 is regarded as a promising option to reduce ferroptosis resistance in the targeted therapy of cancer [8, 32]. The GSH-dependent GPX4 reductive system is a critical anti-ferroptosis pathway [33], which can be induced by cystine when stimulated by P53 or erastin. In this study, we revealed that the MDA content as well as the Ptg2 and 4-HNE protein levels were lower in LUAD tissues, suggesting that ferroptosis resistance in LUAD. Erastin was used to induce ferroptosis of LUAD cells, which upregulated the Ptg2 expression and 4-HNE concentration while decreasing LUAD cell viability. Moreover, the expression

GPX4 was found to be negatively modulated by circSCUBE3. The results of rescue assays also indicated that GPX4 knockdown reversed the effects of circSCUBE3 silencing on the viability and ferroptosis of LUAD cells, which indicated that circSCUBE3 promoted ferroptosis in LUAD by downregulating GPX4.

CREB is previously reported to promote the transcription of GPX4 to repress the ferroptosis in LUAD [11]. A study also reports that CREB is activated by PCTR1 to elevate GPX4 expression in ferroptosis in LPS-induced acute lung injury [34]. In the current work, we elucidated that circSCUBE3 interacted with CREB in LUAD cells and suppressed the binding between CREB and GPX4 promoter as well as the CREB-mediated transcription of GPX4. Additionally, the expression of CREB was not significantly regulated by circSCUBE3. The inhibitory impact induced by CREB silencing on the GSH synthesis in LUAD cells was demonstrated to be reversed by overexpressing GPX4. The results indicated that CREB was required in circSCUBE3-mediated regulation on GPX4.

In conclusion, we confirmed the downregulation and explored the role of circSCUBE3 in ferroptosis of LUAD for the first time. CircSCUBE3 facilitates ferroptosis and decreases the viability and tumorigenesis in LUAD by binding to CREB to downregulate GPX4. The findings of this study might provide novel therapeutic options for the LUAD treatment.

Informed Consent

The authors report no conflict of interest.

Availability of data and material

We declared that we embedded all data in the manuscript.

Authors' contributions

FH conducted the experiments and wrote the paper; ZQ conceived, designed the study and revised the manuscript.

Funding

None.

Acknowledgement

We thanked the Shulan (Hangzhou) Hospital for approval of our study.

References

1. Sung H, Ferlay J, Siegel RL, Laversanne M, Soerjomataram I, Jemal A, Bray F (2021) Global cancer statistics 2020: GLOBOCAN estimates of incidence and mortality worldwide for 36 cancers in 185 countries. *CA Cancer J Clin* 71(3):209–249. doi: 10.3322/caac.21660
2. Thai AA, Solomon BJ, Sequist LV, Gainor JF, Heist RS (2021) Lung cancer. *Lancet* 398(10299):535–554. doi: 10.1016/s0140-6736(21)00312-3
3. Zhang C, Zhang J, Xu FP, Wang YG, Xie Z, Su J, et al (2019) Genomic landscape and immune microenvironment features of preinvasive and early invasive lung adenocarcinoma. *J Thorac Oncol* 14(11):1912–1923. doi: 10.1016/j.jtho.2019.07.031
4. Duma N, Santana-Davila R, Molina JR (2019) Non-small Cell Lung cancer: epidemiology, screening, diagnosis, and treatment. *Mayo Clin Proc* 94(8):1623–1640. doi: 10.1016/j.mayocp.2019.01.013
5. Denisenko TV, Budkevich IN, Zhivotovskiy B (2018) Cell death-

- based treatment of lung adenocarcinoma. *Cell Death Dis* 9(2):117. doi: 10.1038/s41419-017-0063-y
6. Stockwell BR, Friedmann Angeli JP, Bayir H, Bush AI, Conrad M, Dixon SJ, et al (2017) Ferroptosis: A regulated cell death nexus linking metabolism, redox biology, and disease. *Cell* 171(2):273–285. doi: 10.1016/j.cell.2017.09.021
 7. Chen X, Li J, Kang R, Klionsky DJ, Tang D (2021) Ferroptosis: machinery and regulation. *Autophagy* 17(9):2054–2081. doi: 10.1080/15548627.2020.1810918
 8. Yang WS, SriRamaratnam R, Welsch ME, Shimada K, Skouta R, Viswanathan VS, et al (2014) Regulation of ferroptotic cancer cell death by GPX4. *Cell* 156(1-2):317–331. doi: 10.1016/j.cell.2013.12.010
 9. Liang C, Zhang X, Yang M, Dong X (2019) Recent progress in ferroptosis inducers for cancer therapy. *Adv Mater* 31(51):e1904197. doi: 10.1002/adma.201904197
 10. Xu T, Ding W, Ji X, Ao X, Liu Y, Yu W, Wang J (2019) Molecular mechanisms of ferroptosis and its role in cancer therapy. *J Cell Mol Med* 23(8):4900–4912. doi: 10.1111/jcmm.14511
 11. Wang Z, Zhang X, Tian X, Yang Y, Ma L, Wang J, Yu Y (2021) CREB stimulates GPX4 transcription to inhibit ferroptosis in lung adenocarcinoma. *Oncol Rep* 45(6):88. doi: 10.3892/or.2021.8039
 12. Tang X, Ren H, Guo M, Qian J, Yang Y, Gu C (2021) Review on circular RNAs and new insights into their roles in cancer. *Comput Struct Biotechnol J* 19:910–928. doi: 10.1016/j.csbj.2021.01.018
 13. Wang C, Tan S, Liu WR, Lei Q, Qiao W, Wu Y, et al (2019) RNA-Seq profiling of circular RNA in human lung adenocarcinoma and squamous cell carcinoma. *Mol Cancer* 18(1):134. doi: 10.1186/s12943-019-1061-8
 14. Zhou WY, Cai ZR, Liu J, Wang DS, Ju HQ, Xu RH (2020) Circular RNA: metabolism, functions and interactions with proteins. *Mol Cancer* 19(1):172. doi: 10.1186/s12943-020-01286-3
 15. Li J, Sun D, Pu W, Wang J, Peng Y (2020) Circular RNAs in cancer: biogenesis, function, and clinical significance. *Trends Cancer* 6(4):319–336. doi: 10.1016/j.trecan.2020.01.012
 16. Huang Q, Guo H, Wang S, Ma Y, Chen H, Li H, et al (2020) A novel circular RNA, circXPO1, promotes lung adenocarcinoma progression by interacting with IGF2BP1. *Cell Death Dis* 11(12):1031. doi: 10.1038/s41419-020-03237-8
 17. Zhou J, Zhang S, Chen Z, He Z, Xu Y, Li Z (2019) CircRNA-ENO1 promoted glycolysis and tumor progression in lung adenocarcinoma through upregulating its host gene ENO1. *Cell Death Dis* 10(12):885. doi: 10.1038/s41419-019-2127-7
 18. Liang Y, Wang H, Chen B, Mao Q, Xia W, Zhang T, et al (2021) circDCUN1D4 suppresses tumor metastasis and glycolysis in lung adenocarcinoma by stabilizing TXNIP expression. *Mol Ther Nucleic Acids* 23:355–368. doi: 10.1016/j.omtn.2020.11.012
 19. Zheng X, Zhang C (2023) The regulation of ferroptosis by noncoding RNAs. *Int J Mol Sci* 24(17):13336. doi: 10.3390/ijms241713336
 20. Li J, Yang J, Zhou P, Le Y, Zhou C, Wang S, et al (2015) Circular RNAs in cancer: novel insights into origins, properties, functions and implications. *Am J Cancer Res* 5(2):472–480.
 21. Su L, Zhao J, Su H, Wang Y, Huang W, Jiang X, Gao S (2022) CircRNAs in lung adenocarcinoma: diagnosis and therapy. *Curr Gene Ther* 22(1):15–22. doi: 10.2174/1566523221666211202095258
 22. Mou Y, Wang J, Wu J, He D, Zhang C, Duan C, Li B (2019) Ferroptosis, a new form of cell death: opportunities and challenges in cancer. *J Hematol Oncol* 12(1):34. doi: 10.1186/s13045-019-0720-y
 23. Zhi Y, Gao L, Wang B, Ren W, Liang KX, Zhi K (2021) Ferroptosis holds novel promise in treatment of cancer mediated by non-coding RNAs. *Front Cell Dev Biol* 9:686906. doi: 10.3389/fcell.2021.686906
 24. Kristensen LS, Andersen MS, Stagsted LVW, Ebbesen KK, Hansen TB, Kjems J (2019) The biogenesis, biology and characterization of circular RNAs. *Nat Rev Genet* 20(11):675–691. doi: 10.1038/s41576-019-0158-7
 25. Yu T, Wang Y, Fan Y, Fang N, Wang T, Xu T, Shu Y (2019) CircRNAs in cancer metabolism: a review. *J Hematol Oncol* 12(1):90. doi: 10.1186/s13045-019-0776-8
 26. Chen W, Fu J, Chen Y, Li Y, Ning L, Huang D, et al (2021) Circular RNA circKIF4A facilitates the malignant progression and suppresses ferroptosis by sponging miR-1231 and upregulating GPX4 in papillary thyroid cancer. *Aging* 13(12):16500–16512. doi: 10.18632/aging.203172
 27. Zhang X, Xu Y, Ma L, Yu K, Niu Y, Xu X, et al (2022) Essential roles of exosome and circRNA_101093 on ferroptosis desensitization in lung adenocarcinoma. *Cancer Commun (Lond)* 42(4):287–313. doi: 10.1002/cac2.12275
 28. Chen S, Zhang Z, Zhang B, Huang Q, Liu Y, Qiu Y, et al (2022) CircCDK14 promotes tumor progression and resists ferroptosis in glioma by regulating PDGFRA. *Int J Biol Sci* 18(2):841–857. doi: 10.7150/ijbs.66114
 29. Tang B, Zhu J, Li J, Fan K, Gao Y, Cheng S, et al (2020) The ferroptosis and iron-metabolism signature robustly predicts clinical diagnosis, prognosis and immune microenvironment for hepatocellular carcinoma. *Cell Commun Signal* 18(1):174. doi: 10.1186/s12964-020-00663-1
 30. Li D, Li Y (2020) The interaction between ferroptosis and lipid metabolism in cancer. *Sig Transduct Target Ther* 5(1):108. doi: 10.1038/s41392-020-00216-5
 31. Sun Y, Zheng Y, Wang C, Liu Y (2018) Glutathione depletion induces ferroptosis, autophagy, and premature cell senescence in retinal pigment epithelial cells. *Cell Death Dis* 9(7):753. doi: 10.1038/s41419-018-0794-4
 32. Wang Y, Zheng L, Shang W, Yang Z, Li T, Liu F, et al (2022) Wnt/beta-catenin signaling confers ferroptosis resistance by targeting GPX4 in gastric cancer. *Cell Death Differ* 29(11):2190–2202. doi: 10.1038/s41418-022-01008-w
 33. Liu M, Kong XY, Yao Y, Wang XA, Yang W, Wu H, et al (2022) The critical role and molecular mechanisms of ferroptosis in antioxidant systems: a narrative review. *Ann Transl Med* 10(6):368. doi: 10.21037/atm-21-6942
 34. Lv Y, Chen D, Tian X, Xiao J, Xu C, Du L, et al (2023) Protectin conjugates in tissue regeneration 1 alleviates sepsis-induced acute lung injury by inhibiting ferroptosis. *J Transl Med* 21(1):293. doi: 10.1186/s12967-023-04111-9